

Charge exchange $\rho^0\pi^+$ photoproduction and implications for searches of exotic meson

Andrei V. Afanasev^{a,b} and Adam P. Szczepaniak^c

^a *Physics Department, North Carolina Central University, Durham, NC 27707*

^b *Thomas Jefferson National Accelerator Facility, Newport News, VA 23606*

^c *Physics Department and Nuclear Theory Center,*

Indiana University, Bloomington, IN 47405

Abstract

We analyze the processes $\vec{\gamma} + p \rightarrow \rho^0\pi^+n$ at low momentum transfer focusing on a possibility of production of an exotic $J^{PC} = 1^{-+}$ meson state. In particular we discuss polarization observables and conclude that linear photon polarization is instrumental for separating of the exotic wave.

PACS number(s): 12.39.Mk, 12.40.Nn, 13.60.Le, 13.88+e

I. INTRODUCTION

Mesons with unusual quantum numbers play an important role in studies of strong QCD and in understanding of the nature of the effective, low energy degrees of freedom. Since, due to their exotic quantum numbers, such mesons cannot be described in terms of the valence quarks alone, they in principle give access to the dynamics of the nonvalence degrees of freedom thus allowing for studies of strong QCD which go beyond the static $Q\bar{Q}$ confinement. Recently significant progress has been made in lattice studies of such states and several new models have been developed. In these models the unconventional structure of exotic mesons is typically associated with dynamical gluons and lattice gives predictions for the spectrum of gluonic excitations in the presence of static $Q\bar{Q}$ sources. In particular the numerical simulations lead to a series of effective, “excited” $Q\bar{Q}$ adiabatic potentials significantly different from that of the ground state “Coulomb+linear”. These higher adiabatic potentials arise from gluonic field configurations which have symmetries

distinct from that of the ground state [1]. The adiabatic potentials can then be used to predict the spectrum of hybrids with heavy quarks.

The structure of hybrids containing light quarks is less known. Lattice simulations estimate the mass of the ground state 1^{-+} state in the range $1.9 - 2$ GeV [2] but unlike the case of heavy hybrids there is not much information available yet about their structure [3]. A number of models have been proposed to address this issue. They primarily differ in the treatment of the gluonic degrees of freedom. There are models which describe gluons as quasi-particles *i.e.* in a similar way to the constituent quarks [4], other, such as the flux tube model [5] associate gluons with collective excitations of a nonrelativistic string as an approximation to the dynamics of the chromoelectric flux between the $Q\bar{Q}$ pair. Finally in the bag model spectrum of the perturbative gluon field inside the bag is obtained by imposing boundary conditions on the bag surface [6]. All these models lead to modest differences in the predictions for the spectrum and decay pattern of exotic mesons. Future precision data on hybrid production will help discriminating between them and give insight into the nonperturbative dynamics of the gluonic field.

The experimental studies have not yet resulted in an unambiguous spectrum of exotic mesons [7]. Nevertheless a number of strong candidates have been established. The most recent published analysis of the data from the E852 collaboration at BNL indicates a presence of an exotic $J^{PC} = 1^{-+}$ signal in the $\rho\pi$ channel of the reaction $\pi^-p \rightarrow \rho^0\pi^-p \rightarrow \pi^+\pi^-\pi^-p$ [8]. The charged P -wave, $(\rho\pi)^\pm$ channel is particularly useful for exotic searches since it has $G = (-)$ and therefore in the absence of a $I = 2$ meson state (which by itself would be interesting), belongs to an isovector multiplet and therefore has exotic quantum numbers. The 3π mass spectrum (from $\rho^0\pi^\pm \rightarrow \pi^+\pi^-\pi^\pm$) is dominated by the $a_1(1270)$, $a_2(1320)$ and $\pi_2(1670)$ mesons. As discussed in Ref. [8] the exotic wave was extracted through partial wave analysis and a state with mass of $1593 \pm 8_{-47}^{+29}$ MeV and width $\Gamma = 168 \pm 20_{-12}^{+150}$ MeV was found to have a resonant behavior.

To the best of our knowledge the only photoproduction experiment claiming a possible exotic signal was performed at the SLAC bubble chamber with laser backscattered 30 GeV electrons producing linearly polarized photons with an average energy $E_\gamma = 19.5$ GeV [9]. The measured 3π mass spectrum looks somewhat different from that produced with the pion beam. Below $M_{3\pi} \sim 1.5$ GeV it is still dominated by the a_2 resonance but there is no clear indication of the a_1 . At higher mass a narrow peak at $M_{3\pi} \sim 1.8$ GeV is seen, rather different from the π_2 seen by the E856 collaboration. A theoretical study of the cross section for the photoproduction of a 1^{-+} exotic was performed in [10] in a flux-tube model and finds it to be of the order of $0.5 \mu b$. This is close in magnitude to the cross section of the $a_2(1320)$, and thus in principle, in photoproduction exotic mesons could be produced at a rate similar to the production of other, non-exotic states [11].

As we discuss below the observed photoproduction spectrum is consistent with theoretical expectations. In particular, with realistic parameters for an 1^{-+} exotic state we find that a signal

from such a state could stand out above the π_2 peak in the 3π mass spectrum. Furthermore we discuss the importance of linear photon polarization in the partial wave analysis and in particular in isolating the exotic meson signal. This is of central importance for the new generation of meson photoproduction experiments proposed in conjunction with the planned energy upgrade at the Jefferson Lab –the Hall D project, where production mechanisms and decay modes of various meson states could be studied with high precision [12]. The paper is organized as follows. Below we discuss the formalism used to describe the photoproduction mechanisms and the treatment of the production of the produced $\rho\pi$ pair. In Section. III we present our numerical results, and summarize our conclusions in Section. IV.

II. FORMALISM

The process under investigation is $\vec{\gamma}p \rightarrow X^+n \rightarrow (\rho^0\pi^+)n$ and it is shown in Fig. 1. At high photon lab energy, $E_\gamma > \text{few GeV}$ and low momentum transfer, $t = (p'_N - p_N)^2$, photoproduction is dominated by peripheral production off the meson cloud around the proton target. Due to proximity of the pion pole, in a charge exchange reaction one expects one-pion-exchange (OPE) to dominate the production amplitude. As discussed in more detail in Section III, this seems to be supported by the existing data and therefore we will specialize our analysis to this particular case even though the formalism can be easily extended to account for other production mechanisms. One objective of our study will then be to explore the consequences of the unnatural parity exchange (naturalness τ of a particle with spin J and intrinsic parity η is defined as $\tau = \eta(-)^J$), for polarization observables.

The differential cross section for $\vec{\gamma}p \rightarrow X^+n \rightarrow (\rho^0\pi^+)n$ is given by

$$\frac{d^2\sigma}{dt dM_{\rho\pi} d\Omega_k} = \frac{1}{2} \sum_{\lambda_N \lambda_{N'}} \frac{389.3 \mu\text{b GeV}^2}{64\pi m_N^2 E_\gamma^2} \frac{|\mathbf{k}_\rho|}{2(2\pi)^3} |A(s, t, M_{\rho\pi}, \lambda_\gamma \lambda_N \lambda'_N \lambda_\rho)|^2. \quad (1)$$

Here \mathbf{k}_ρ is the 3-momentum of the ρ^0 in the $(\rho^0\pi^+)$ c.m.s., $|\mathbf{k}_\rho| = \lambda(M_{\rho\pi}, m_\rho, m_\pi)$ and A is the reduced photoproduction amplitude. Processes dominated by a t -channel meson exchange are simplest to analyze in the Gottfried-Jackson, (GJ) frame defined as the rest frame of the produced resonance, X^+ (and thus also the $\rho^0\pi^+$ system) with the z axis defined along the direction of the photon momentum and y perpendicular to the $\gamma p \rightarrow Xn$ production plane (see Fig. 2). The spin structure of the photoproduction amplitude $A(s, t, M_{\rho\pi}, \lambda_\gamma \lambda_N \lambda'_N \lambda_\rho)$ is in general described in terms of 12 independent complex amplitudes, *i.e.* 23 real functions, however, in the OPE approximation the amplitude A reduces to

$$A = A_{OPE}(s, t) \delta_{\lambda_N, -\lambda'_N} T(M_{\rho\pi}, t, s, \lambda_\rho \lambda_\gamma). \quad (2)$$

Here

$$A_{OPE}(s, t) = \sqrt{2}g_{\pi NN} \left(\frac{s}{s_0}\right)^{\alpha_\pi(t)} \frac{\sqrt{t'}}{(t - m_\pi^2)}, \quad (3)$$

with $s = 2E_\gamma m_N + m_N^2$, $\alpha_\pi(t) = 0.9 \text{ GeV}^{-2}(t - m_\pi^2)$ and the factor of $\sqrt{t'} \equiv \sqrt{|t - t_{\min}|}$ comes from the helicity flip πNN vertex proportional to the πNN coupling given by $g_{\pi NN}^2/4\pi = 14.4$. The amplitude T should be extrapolated off the pion mass shell which together with absorption corrections will modify the overall t -dependence. We will discuss this in Section III. The OPE approximation leaves only the amplitude $T(M_{\rho\pi}, t, s, \lambda_\rho \lambda_\gamma)$ to be described phenomenologically. Its spin structure is significantly simplified, with only 3 independent helicity amplitudes (or 5 real functions) to be determined from measurements. One can demonstrate that magnitudes of all of these amplitudes can be extracted from double polarization observables using a linearly polarized photon beam and measuring linear polarization of the final ρ . It should be noted that since the spinless particle is exchanged in the t -channel, there is no correlation between the photon and nucleon spins.

The amplitude $T = T(\gamma\pi^+ \rightarrow \rho^0\pi^+)$ will be constructed below assuming a single resonance dominates a given J^{PC} channel of the $(\rho^0\pi^+)$ system. Phenomenologically, this is expected to be the case for $1 \text{ GeV} < M_{\rho\pi} < 2 \text{ GeV}$ where the $\rho^0\pi^+$ spectrum seems to be saturated by the $a_1(J^P = 1^+)$, $a_2(J^P = 2^+)$, and $\pi_2(J^P = 2^-)$ resonances. Nevertheless, the formalism developed below can be easily generalized to include other states and possibly a nonresonant background.

A. Unitary model for the $\vec{\gamma}\pi^+ \rightarrow \rho^0\pi^+$ amplitude

In order to be able to reproduce full widths of the hadronic resonances contributing to the production of the $\rho^0\pi^+$ pair we have

to take into account hadronic states other than just the $\rho\pi$. Fortunately, all of the states listed above have typically at most two dominant decay channels and they all correspond to two meson states. For example, almost 100% of the a_1 width comes from coupling to the $\rho\pi$ channel. The a_2 decays are also dominated by the $\rho\pi$ mode (70%) followed by the $\eta\pi$ mode (15%). Finally for π_2 the ratios are, 56% for the $f_2\pi$ decay channel and 31% for the $\rho\pi$ [13]. To keep the model simple we will therefore truncate the hadronic Fock space and include a single resonance state $|X\rangle$, and up to two, two-body meson channels, $|AB\rangle$, one corresponding to the measured $\rho^0\pi^+$ state and the other specific to the particular resonance, as listed above. We also introduce a $J^{PC} = 1^{-+}$ exotic state and later present numerical results for different choices of its mass and width.

In model calculations, an exotic state with a mass below 2 GeV is predicted to couple mainly to the $b_1\pi$ and $f_2\pi$ followed by the $\rho\pi$ channels. The E852 data, however, have so far only seen the exotic wave in the $\rho\pi$ channel [8]. It is possible that final state interactions shift the strength between the different channels and make the couplings to the $\rho\pi$ and the $b_1\pi$ channels comparable.

We will thus make a crude assumption that decays of the exotic are dominated by a single S -wave channel (*e.g.* the $(b_1\pi)_S$) and a single P -wave in the $(\rho\pi)_P$ channel each contribution roughly 50% to the total hadronic width. The full list of channels used in this study is summarized in Table 1.

With the assumptions given above, and ignoring final state interaction (which for example could be incorporated into the scattering matrix in a form of Blatt-Weisskopf factors) the model is completely specified by a Hamiltonian which in the rest frame of the resonance is given by

$$H = M + \delta M + K + V^s + V^e. \quad (4)$$

For the simple channel interactions described above it is also possible to write a manifestly Lorentz invariant expression for the resulting S -matrix. We choose to work with a fixed frame Hamiltonian formalism to enable a simple connection with other noncovariant models, *e.g.* quark model, flux tube model or bag model where most of the calculations for the channel couplings, especially involving hybrids have been made. In Eq. (4) the first term represents the kinetic energy of a resonance with a physical mass $M|X\rangle = m_X|X\rangle$ and the bare mass $(M + \delta M)|X\rangle = (m_X + \delta m_X)|X\rangle \equiv \bar{m}_X|X\rangle$. The second term is the kinetic energy of the two mesons $K|AB, \mathbf{k}\rangle = (\sqrt{m_A^2 + \mathbf{k}^2} + \sqrt{m_B^2 + \mathbf{k}^2})|AB, \mathbf{k}\rangle$ with \mathbf{k} being the relative 3-momentum between the two mesons in their rest frame. The potentials V^s and V^e describe strong and electromagnetic couplings between the resonance X and the two-meson states, respectively. The mass shifts δm_X will be adjusted to match positions of the maxima of the scattering amplitude T with the physical masses, m_X of the resonances, and the strong couplings specifying V^s will be fixed by the phenomenological strong partial widths of the resonances. With absence of other channels coupled to the two-meson state there are no mass shifts to m_A or m_B . Also, to first order in the electromagnetic interactions the strength of V^e can be directly calculated from the $X \rightarrow \gamma\pi$ decay widths.

We will first discuss the electromagnetic interactions. The truncated matrix elements of V^e (*e.g.* with the total 3-momentum conserving δ -functions eliminated) in the resonance rest frame are given by

$$\langle \gamma\pi; \mathbf{q}, \lambda_\gamma | V^e | X; J^P, \lambda_X \rangle = \sum_{L_\gamma} (m_X g_{X\gamma\pi}^{L_\gamma}(q)) \left(\frac{q}{m_X} \right)^{L_\gamma} V_{J^P L_\gamma}^e(\hat{\mathbf{q}}, \lambda_X, \lambda_\gamma), \quad (5)$$

where \mathbf{q} is the photon momentum in the $\gamma\pi$ rest frame, $q = |\mathbf{q}|$, λ_γ is the photon helicity, and the resonance spin, λ_X is quantized along the \mathbf{z} axis. Furthermore, $V_{J^P L_\gamma}^e = \sum_\lambda \sqrt{\frac{2L_\gamma+1}{4\pi}} \langle J_X \lambda_X | L_\gamma 0, 1\lambda \rangle D_{\lambda\lambda_\gamma}^{J_X}(\hat{\mathbf{q}})$ and the Wigner rotation takes care of the possible difference in the direction of photon polarization and spin quantization axis if the photon momentum is not parallel to the later. In the GJ frame, however, $\mathbf{q} = q\hat{\mathbf{z}}$ and the Wigner rotation becomes trivial, $D_{\lambda\lambda_X}^{J_X}(\hat{\mathbf{z}}) = \delta_{\lambda\lambda_X}$. The momentum dependence of the electromagnetic couplings, $g_{X\gamma\pi}^{L_\gamma}(q)$ could be calculated in a given microscopic model.

The matrix elements of the strong interaction potential are given by

$$\langle X; J^P, \lambda_X | V^s | AB; \mathbf{k}, s_A \lambda_A, s_B \lambda_B \rangle = \sum_{L_{AB}} (\bar{g}_{XAB}^{L_{AB}}(k) m_X) \left(\frac{k}{m_X} \right)^{L_{AB}} V_{J^P L_{AB}}^s(\hat{\mathbf{k}}, \lambda_X s_A s_B \lambda_A \lambda_B), \quad (6)$$

with $V_{J^P L_{AB}}^s = \sum_{M_{AB} s_{AB} \lambda_{AB}} \langle s_{AB} \lambda_{AB} | s_A \lambda_A, s_B \lambda_B \rangle \langle s_{AB} \lambda_{AB}, L_{AB} M_{AB} | J \lambda_X \rangle Y_{L_{AB} M_{AB}}(\hat{\mathbf{k}})$. We choose a simple parameterization of the momentum dependence of the bare couplings $\bar{g}_{XAB}^L(k) = \bar{g}_{XAB}^L \exp(-k^2/\Lambda^2)$ with $\Lambda = O(1 \text{ GeV})$. It will be convenient to define $q(M) \equiv \lambda(M, 0, m_\pi)$ and $k_{AB}(M) \equiv \lambda(M, m_A, m_B)$ which represent the breakup momenta of the $\gamma\pi$ and of the AB system respectively coming from a decay of a state with mass M .

The $\gamma\pi \rightarrow AB$ scattering amplitude, T is obtained from the solution of the Lippmann-Schwinger equation for the Hamiltonian in Eq. (4) and it is given by,

$$\langle \gamma\pi; \mathbf{q}, \lambda_\gamma | T(E) | AB; s_A \lambda_A, s_B \lambda_B \rangle = \sum_{X; J^P \lambda_X L_\gamma L_{AB}} V_{J^P L_\gamma}^e(\mathbf{q}, \lambda_X, \lambda_\gamma) T_{X, J^P}^{L_\gamma L_{AB}}(E) V_{J^P L_{AB}}^s(\mathbf{k}, \lambda_X s_A s_B \lambda_A \lambda_B), \quad (7)$$

with

$$T_{X, J^P L_\gamma L_{AB}}(E) = \left(\frac{q}{m_X} \right)^{L_\gamma} \frac{m_X g_{X\gamma\pi}^{L_\gamma}(q) \bar{g}_{XAB}^{L_{AB}}(k)}{2 \left(E - m_X - \Sigma_{X, J^P}(E) + i \frac{\Gamma_{X, J^P}(E)}{2} \right)} \left(\frac{k}{m_X} \right)^{L_{AB}}, \quad (8)$$

where the energy dependent shifts in the real part are given by

$$\begin{aligned} \Sigma_{X, J^P}(E) &= \sum_{AB, L_{AB}} \frac{(\bar{g}_{XAB}^{L_{AB}}(k_{AB}(m_X)) m_X)^2}{64\pi^3} \\ &\times \mathcal{P} \int_{m_A+m_B}^d M \frac{dM}{M} \left(\frac{k_{AB}(M)}{m_X} \right)^{2L_{AB}+1} \left(\frac{\bar{g}_{XAB}^{L_{AB}}(k_{AB}(E))}{\bar{g}_{XAB}^{L_{AB}}(k_{AB}(m_X))} \right)^2 \left(\frac{1}{E-M} - \frac{1}{m_X-M} \right). \end{aligned} \quad (9)$$

The second term under the integral comes from the δm_X mass counter-term chosen so that $\Sigma(m_X) = 0$ making the real part of T vanish at the position of the resonance. The energy dependent widths are

$$\begin{aligned} \Gamma_{X, J^P}(E) &= \sum_{AB, L_{AB}} \Gamma_{X, J^P}^{L_{AB}}(E) = \sum_{AB, L_{AB}} m_X \frac{(\bar{g}_{XAB}^{L_{AB}}(k_{AB}(E)))^2 m_X}{32\pi^2 E} \left(\frac{k_{AB}(E)}{m_X} \right)^{2L_{AB}+1} \\ &= \sum_{AB, L_{AB}} \Gamma_{X, J^P}^{BW, L_{AB}} \left(\frac{k_{AB}(E)}{k_{AB}(m_X)} \right)^{2L_{AB}+1} \frac{m_X}{E} \left(\frac{\bar{g}_{XAB}^{L_{AB}}(k_{AB}(E))}{\bar{g}_{XAB}^{L_{AB}}(k_{AB}(m_X))} \right)^2, \end{aligned} \quad (10)$$

where $\Gamma_{X, J^P}^{BW, L_{AB}}$ is the Breit-Wigner (BW) width of the resonance X decaying into a two-body hadronic state AB in the L_{AB} partial wave. The physical, $g_{XAB}^{L_{AB}}$ and bare couplings, $\bar{g}_{XAB}^{L_{AB}}$ are related by

$$g_{XAB}^{L_{AB}} = \frac{\bar{g}_{XAB}^{L_{AB}}}{\left[1 - \left(\frac{d}{dE} \Sigma_{X, J^P}(E) \right)_{E=m_X} \right]^{1/2}}, \quad (11)$$

so that near the resonance pole $T_X(E)$ has the BW form,

$$T_{X,J^P L_\gamma L_{AB}}(E \sim m_X) = \left(\frac{q(m_X)}{m_X} \right)^{L_\gamma} \frac{m_X g_{X\gamma\pi}^{L_\gamma}(q_X) g_{XAB}^{L_{AB}}(k_X)}{2 \left(E - m_X + i \frac{\Gamma_{X,J^P}^{BW}}{2} \right)} \left(\frac{k_{AB}(m_X)}{m_X} \right)^{L_{AB}}. \quad (12)$$

Table 2 lists the numerical values of the bare and physical couplings obtained for the set of resonance parameters given in Table 1. For the $AB = \rho^0 \pi^+$ final state, the unpolarized differential cross section integrated over the solid angle Ω_k in the GJ frame is then given by

$$\frac{d^2\sigma}{dt dM_{\rho\pi}} = \frac{389.3 \mu\text{b GeV}^2}{4m_N^2 E_\gamma^2} |A_{OPE}(s, t)|^2 \frac{M_{\rho\pi}}{q} \sum_{X,J^P} \frac{m_X \Gamma_{X \rightarrow \gamma\pi}(q(M_{\rho\pi})) \Gamma_{X \rightarrow \rho^0 \pi^+}^{L_{\rho\pi}}(k_{\rho\pi}(M_{\rho\pi}))}{(M_{\rho\pi} - m_X - \Sigma_{X,J^P}(M_{\rho\pi}))^2 + \left(\frac{\Gamma_{X,J^P}(M_{\rho\pi})}{2} \right)^2}. \quad (13)$$

The energy dependent electromagnetic widths are calculated from,

$$\Gamma_{X \rightarrow \gamma\pi}(E) = m_X \sum_{L_\gamma, L'_\gamma} \frac{g_{X\gamma\pi}^{L_\gamma}(q(E)) g_{X\gamma\pi}^{L'_\gamma}(q(E))}{32\pi^2} \left(\frac{q(E)}{m_x} \right)^{L_\gamma + L'_\gamma + 1} \\ \times \left[\delta_{L_\gamma, L'_\gamma} \left(\delta_{L_\gamma, J} + \delta_{L_\gamma, J+1} \frac{J}{2J+1} + \delta_{L_\gamma, J-1} \frac{J+1}{2J+1} \right) + \left(\delta_{L_\gamma, J+1} \delta_{L'_\gamma, J-1} + \delta_{L'_\gamma, J+1} \delta_{L_\gamma, J-1} \right) \frac{\sqrt{J(J+1)}}{2J+1} \right]. \quad (14)$$

To account for the kinematics of the off-shell pion in the t -channel we replace the momentum $q(M_{\rho\pi})$ in the the angular momentum factors, by $q(M_{\rho\pi}) = \lambda(M_{\rho\pi}, 0, m_\pi) \rightarrow \lambda(M_{\rho\pi}, 0, t)$. We however, keep the on-shell $q(M_{\rho\pi})$ in the argument of the couplings, $g_{X\gamma\pi}^{L_\gamma}(q(E))$. We will further study the resulting t -dependence of the full photoproduction amplitude in Section III.

Unlike the case of strong decays considered here, in radiative decays (to real photons), L_γ is not a good quantum number and as seen from Eq. (14), if more then one partial amplitude contributes the radiative width, $\Gamma_{X \rightarrow \gamma\pi}$ does not determine the individual electromagnetic couplings $g_{X\gamma\pi}^{L_\gamma}$ but only a linear combination of products. In the case considered here a_1 and π_2 have more then one partial wave contributing to the $\gamma\pi$ decay, the $S + D$ and $P + F$ waves respectively. We will fix the ratio of these amplitudes to match the ratio of the corresponding waves in the $X \rightarrow \rho\pi$ decays as in the VMD model.

B. Polarization observables

It is well known that linear polarization gives access the the largest possible number of independent production amplitudes. Even more importantly, however, linear polarization is necessary

for isolating t -channel natural from unnatural parity exchanges [14]. This follows from transformation properties of the production amplitude under parity which relates amplitudes with opposite helicities and depends on the naturalities of particles involved in the process. It then follows that in order to be able to discriminate between different naturalities it is necessary to have a *coherent* superposition of helicity states, which in the case of real photons corresponds to linear, or more generally elliptical polarization. Alternatively, if the naturality of the t -channel exchange is presumed to be known, as in the case studied here, parity arguments imply that the correlation between polarization direction of the photon and that of the produced mesonic resonance will depend on the naturality of the produced resonance. The proof is straightforward. Consider the matrix element of the electromagnetic interaction V^e given in Eq. (5). Parity invariance restricts the possible values of L_γ so that $(-1)^{L_\gamma} = \eta_X$, where η_X is the intrinsic parity of the resonance. From the properties of the CG coefficients it follows that such a matrix element satisfies,

$$V_{J^P L_\gamma}^e(\lambda_\gamma, \lambda_X) = (-1)^{J_X + L_\gamma + 1} V_{J^P L_\gamma}^e(-\lambda_\gamma, -\lambda_X) = -\tau_X V_{J^P L_\gamma}^e(-\lambda_\gamma, -\lambda_X), \quad (15)$$

where $\tau_X = \eta_X (-1)^{J_X}$ is the naturality of the resonance.

A photon beam linearly polarized either along \mathbf{y} *i.e.* perpendicular to the production plane or along $\mathbf{x} = \mathbf{y} \times \mathbf{z}$ corresponds to an initial state $|i\rangle$, $i = \mathbf{x}, \mathbf{y}$ which is a linear superposition of helicity states $|\lambda_\gamma\rangle$, $\lambda_\gamma = \pm 1$,

$$|\mathbf{x}\rangle = \frac{1}{\sqrt{2}} (|-1\rangle - | +1\rangle), \quad |\mathbf{y}\rangle = \frac{i}{\sqrt{2}} (|-1\rangle + | +1\rangle), \quad (16)$$

Introduction a similar basis to describe the orientation of the linear polarization of the resonance and rewriting the matrix elements of $V_{J^P L_\gamma}^e$ given by Eq. (15) in this basis leads to

$$V_{J^P L_\gamma}^e(\mathbf{x}_\gamma, \mathbf{x}_X) = V_{J^P L_\gamma}^e(\mathbf{y}_\gamma, \mathbf{y}_X) \neq 0, \quad V_{J^P L_\gamma}^e(\mathbf{y}_\gamma, \mathbf{x}_X) = V_{J^P L_\gamma}^e(\mathbf{x}_\gamma, \mathbf{y}_X) = 0, \quad (17)$$

if the produced resonance is unnatural ($\tau_x = -1$) and

$$V_{J^P L_\gamma}^e(\mathbf{y}_\gamma, \mathbf{x}_X) = V_{J^P L_\gamma}^e(\mathbf{x}_\gamma, \mathbf{y}_X) \neq 0, \quad V_{J^P L_\gamma}^e(\mathbf{x}_\gamma, \mathbf{x}_X) = V_{J^P L_\gamma}^e(\mathbf{y}_\gamma, \mathbf{y}_X) = 0, \quad (18)$$

if it is natural ($\tau_X = +1$), respectively. In other words, if OPE dominates production the direction of linear polarization of the produced resonance will be parallel to that of the incoming photon if the produced resonance is unnatural and perpendicular if it is natural. As will be shown below this provides an important tool for isolating the produced resonances.

Polarization observables may simplify due to simple spin structure of OPE. In particular, one may show from parity arguments that the photons polarized perpendicular to the production plane (*i.e.*, along y -axis), would not lead to linear polarization of the final ρ along z -direction. This would not be true if a vector particle is exchanged in t -channel.

The measurement of the direction of linear polarization of the resonance requires analysis of the angular distribution of its decay products. Recall that in the case of a vector resonance decaying into two (pseudo)scalars the so called Σ asymmetry is introduced to measure the degree of linear polarization of the vector meson. It is defined as

$$\Sigma = \frac{W_{\mathbf{y}}(\frac{\pi}{2}, \frac{\pi}{2}) - W_{\mathbf{x}}(\frac{\pi}{2}, \frac{\pi}{2})}{W_{\mathbf{y}}(\frac{\pi}{2}, \frac{\pi}{2}) + W_{\mathbf{x}}(\frac{\pi}{2}, \frac{\pi}{2})} \quad (19)$$

where the intensities $W_i(\theta_k, \pi_k)$ come from the photons polarized in the direction $i = \mathbf{x}, \mathbf{y}$ and θ_k and ϕ_k are the decay angles representing direction of flight of one of the two (pseudo)scalars, $\mathbf{k} = k(\sin \theta_k \cos \phi_k, \sin \theta_k \sin \phi_k, \cos \theta_k)$ in the GJ frame. The decay amplitude of a spin-1 resonance linearly polarized along $i_X = \mathbf{x}_X, \mathbf{y}_X$ to two (pseudo)scalars is proportional to $\sum_{\lambda_X=\pm 1} \epsilon^{i_X}(\lambda_X) Y_{1,\lambda_X}(\theta_k, \phi_k)$ where $\epsilon(\lambda_X)$ is the resonance polarization vector. This results in an amplitude proportional to k^x or k^y for vector mesons polarized along \mathbf{x} and \mathbf{y} respectively. In other words, vector meson 100% polarized along the \mathbf{x} or \mathbf{y} direction leads to an intensity of the decay products picking along \mathbf{x} or \mathbf{y} direction respectively. If the correlation between photon and resonance polarization comes from Eq. (18) (*i.e.* a natural resonance is produced via an unnatural t -channel exchange *e.g.* OPE) then polarization of the vector meson is perpendicular to that of the photon. Since Σ refers to decay distributions measured along \mathbf{y} ($\theta_k = \phi_k = \pi/2$) a nonvanishing contributions comes from photons polarized along \mathbf{x} resulting in $\Sigma = -1$. Alternatively, if production is via a natural exchange (*e.g.* Pomeron) then vector meson polarization is parallel to that of the photon and non-vanishing Σ comes from photons polarized along \mathbf{y} resulting in $\Sigma = +1$. In the general case when both natural and unnatural t -channel exchanges take place simultaneously, in vector meson production Σ asymmetry can be used to discriminate between the two mechanisms.

In the case under study, the photoproduced resonance decays into a vector (ρ^0) and a pseudoscalar (π^+) and it is necessary to generalize the definition of the asymmetry in order to reflect the correlation between photon and resonance polarizations. The $\rho^0\pi^+$ decay distribution depends on the polarization of the ρ^0 , which in turn is reflected in the angular distribution of the $\pi^+\pi^-$ from its decay. Thus it is best to study a distribution which correlates the direction of the relative momentum, \mathbf{k} between the ρ^0 and the π^+ coming from the decay of the photoproduced resonance and the direction the relative momentum, \mathbf{p} (measured in the rest frame of the ρ^0) between the two pions from the ρ^0 decay. To obtain the amplitude T describing the $\pi^+\pi^-\pi^+$ production we multiply the amplitude in Eq. (8) (for $AB = \rho^0\pi^+$) by $\mathbf{p}\epsilon(\lambda_{\rho^0})/\sqrt{2}$ corresponding to a BW approximation to the ρ^0 propagator (the factor of $\sqrt{2}$ coming from the isospin). Summing over λ_{ρ^0} allows to express the 3π photoproduction in terms of the four angles θ_k, ϕ_k , and θ_p, ϕ_p specifying the directions of $\hat{\mathbf{k}}$ and $\hat{\mathbf{p}}$ respectively. In Table 3 we give the analytical forms of these dependencies for the resonances considered here. Inspecting the formulas in Table 3 it follows that in

particular measuring $d\sigma/dM_{3\pi}d\Omega_p d\Omega_k$ at $\theta_p = \pi/4$, $\phi_p = \pi/2$ and $\theta_k = \pi/4$, $\phi_k = 3\pi/4$ eliminates contribution from the π_2 resonance. Thus if the exotic state is weakly produced near the π_2 mass region linearly polarized photons enable to enhance the signal in the partial wave analysis.

III. NUMERICAL RESULTS

We first discuss the momentum transfer dependence of $d\sigma/dt$. The existing data on $\rho^0\pi^+$ photoproduction in the mass region of interests, ($1 \text{ GeV} < M_{3\rho^0\pi^+} < 2 \text{ GeV}$), comes from two, SLAC experiments [9,15]. The measurement of Eisenberg *et al.* was performed at two photon energies, $E_\gamma = 4.3$ and 5.25 GeV . Reconstructed 3π mass spectrum shows a clear signature of the a_2 resonance and a broad enhancement in the mass region of $M_{3\pi} = 1.5 - 2 \text{ GeV}$. The total a_2 photoproduction cross section, (averaged over the two photon energies) was found to be $0.9 \pm 0.6\mu b$. This, however, as pointed out in Ref. [9], does not account for other decay modes of the a_2 correcting for which gives $\sigma(\gamma p \rightarrow a_2^+ n) = 2.6 \pm 0.6\mu b$ at $E_\gamma = 4.8 \text{ GeV}$. In Ref. [15] the momentum transfer dependence has been fitted to OPE with absorption corrections corresponding to final state $a_2 n$ scattering. These corrections have been calculated using the strong cutoff model (SCM) where partial waves of the OPE amplitude are cut from below and contributions from waves with $J < J_c$ are eliminated. The cutoff parameter, J_c was fitted to data and found to correspond to an absorption radius of $\sim 1 \text{ fm}$. The second experiment of Condo *et al.* measured the $\rho^0\pi^+$ photoproduction at the average photon energy of $E_\gamma = 19.5 \text{ GeV}$ and for the total a_2^+ photoproduction cross section finds $\sigma(\gamma p \rightarrow a_2^+ n) = 0.29 \pm 0.09\mu b$. At these higher photon energies t -dependence was also found to be consistent with OPE, and it was parameterized with a single exponential form, $d\sigma/dt \propto \exp(bt)$ with $b \sim 10 \text{ GeV}^{-2}$.

In Fig. 3 we show the results of the different parameterizations of the t -dependence in the a_2^+ mass region at $E_\gamma = 4.8 \text{ GeV}$ as compared to the data from Ref. [15], and rescaled as described above. To account for the absorption corrections we have replaced the OPE amplitude of Eq. (3) by

$$A_{OPE}(s, t) \rightarrow A_{OPE}(s, t)T_{cor}(t), \quad (20)$$

with the correction term parameterized by

$$T_{cor}(t) = (a_1 e^{b_1 t} + a_2 e^{b_2 t})^{1/2}. \quad (21)$$

To obtain the a_2^+ photoproduction cross section we have integrated the differential cross section $d\sigma/dtdM_{\rho^0\pi^+}$ calculated using the formalism described in Sec.II over the a_2 mass region corresponding to the data of Ref. [15], *i.e* $M_{a_2^+} - \Gamma/2 < M_{\rho^0\pi^+} < M_{a_2^+} + \Gamma/2$ with $M_{a_2} = 1.31 \text{ GeV}$ and $\Gamma = 80 \text{ MeV}$. The parameters entering in Eq. (21) have been chosen to give the best description of

the $E_\gamma = 4.8$ GeV and the $E_\gamma = 19.5$ GeV data of Condo *et al.*, leading to $\sigma(\gamma p \rightarrow a_2^+) = 1.92\mu b$ and $\sigma(\gamma p \rightarrow a_2^+ n) = 0.43\mu b$ for the two energies respectively. This corresponds to $b_1 \sim 35\text{GeV}^{-1}$, $b_2 \sim 3\text{GeV}^{-2}$, $a_1 \sim 30.0$ and $a_2 \sim 1.5$ for $\Lambda = 1$ GeV. The t dependence at $E_\gamma = 4.8$ GeV is shown by the solid line in Fig. 3. The calculation at the higher energy takes into account the energy dependence of the OPE amplitude as well as the different a_2^+ mass region quoted in Ref. [9], $M_{a_2} = 1.325$ GeV and $\Gamma = 150$ MeV. We have also studied dependence of the form factor scale Λ . For smaller cutoff we find that it becomes harder to simultaneously reproduce the cross sections at both energies 4.8 and 19.5 GeV. Specifically, for $\Lambda = 0.5$ GeV the predictions are $\sigma = 1.86\mu b$ and $\sigma = 0.46\mu b$ respectively. On the other hand for cutoff larger than 1GeV our simple model with one resonance in a given partial wave becomes inadequate as indicated by a rapid increase of the mass shifts $\bar{m}_X - m_X \sim 300 - 500\text{MeV}$. In Fig. 3 we also show $d\sigma/dt$ calculated with the pure OPE amplitude (*i.e.* using $T_{cor} = 1$) (dashed line). Finally the straight dotted line corresponds to the parameterization of Condo *et al* *i.e.* with a replacement

$$A_{OPE} \rightarrow A e^{bt/2} \quad (22)$$

with $b \sim 10\text{GeV}^{-2}$ and normalized to match to total cross section calculated with T_{cor} of Eq. (21).

From the results in Fig. 3 it is clear that the single exponential does not reproduce the entire t -dependence as good as the two-exponential parameterization of Eq. (21) indicating that the absorption corrections are indeed significant. We should stress, however, that the form given in Eq. (21) is only a parameterization and does not correspond to a particular absorption model. In fact as seen from Fig. 3 at low- t the data is above the OPE prediction by a factor of 2–3 *i.e.* $T_{cor} > 1$ while for a truly absorptive correction one should have $T_{cor} < 1$. Using a specific absorption model *e.g.* SCM, $T_{cor} < 1$ is obtained automatically but then to reproduce the magnitude of the cross section requires couplings (*e.g.* $g_{a_2\gamma\pi}$) significantly larger than quoted by the PDG [13]. This is in fact what happens with the fit in Ref. [15] where the extracted $\Gamma_{a_2 \rightarrow \gamma\pi}$ is larger than used here by almost a factor of two. Furthermore the form of OPE cross section used in Ref. [15] is enhanced at low t since it was chosen proportional to t rather than t' , which all together makes the the fit to their data possible with an absorption term, $T_{cor} < 1$. More precise data is clearly needed to resolve these discrepancies.

In the following we will continue with the parameterization of Eq. (21) with the set of parameters listed above. In Fig. 4 we show the mass dependence of $d\sigma/dM_{\rho^0\pi^+}$ when only the single a_2^+ resonance is retained in the photoproduction amplitude. The upper solid line uses $\Lambda = 1$ GeV and the dashed line which is lower at larger $M_{\rho^0\pi^+}$ is the corresponding BW approximation. The second solid line and the corresponding BW approximation (dashed line) correspond to $\Lambda = 0.5$ GeV. In Fig. 5 we give the full prediction of the model *i.e.* with all resonances included. In Fig. 5a the $J^{PC} = 1^{-+}$ resonance mass has been set at $M = 1.775$ GeV which corresponds to the Condo state, and the different plots correspond to $\Gamma = 100$ MeV and $\Gamma^e = 400$ keV (upper

solid line), $\Gamma = 100$ MeV and $\Gamma^e = 200$ keV (lower solid line), $\Gamma = 200$ MeV and $\Gamma^e = 400$ keV (upper dashed line), $\Gamma = 200$ MeV and $\Gamma^e = 200$ keV (lower solid line). In Fig. 5b we set $M_{1^-+} = 1.6$ GeV as measured by the E852 collaboration, with $\Gamma = 170$ MeV and $\Gamma^e = 400$ keV (solid line), $\Gamma^e = 600$ keV (dotted line), and $\Gamma^e = 200$ keV (dashed line). Finally in Fig. 6 we show the sensitivity to the degree of photon linear polarization defined as

$$\delta \frac{d\sigma}{dM_{\rho^0\pi^+}d\Omega_k d\Omega_p} = \frac{1}{P_\gamma} \left(\frac{d\sigma_y}{dM_{\rho^0\pi^+}d\Omega_k d\Omega_p} - \frac{d\sigma_x}{dM_{\rho^0\pi^+}d\Omega_k d\Omega_p} \right) \quad (23)$$

where the subscript in σ refers to the direction of the photon polarization and $0 \leq P_\gamma \leq 1$ is the degree of linear polarization. In Fig. 6a we choose $|k_x| = |k_y|$, $\hat{\mathbf{p}} \cdot \hat{\mathbf{k}} = 0$ and $\theta_p = 0.35\pi$. It follows from the angular distributions listed in Table 3, that at these angles contributions to the asymmetry from $|\pi_2|^2$ and $|a_1|^2$ identically vanish leaving only the a_2 and 1^-+ intensities together with all interference terms. The solid line is the full calculation with all resonances included while the dashed line has the 1^-+ exotic state removed. In Fig. 6b choosing $\theta_p = \pi/4$, $\phi_p = \pi/2$, $\theta_k = \pi/4$, $\phi_k = 3\pi/4$ which leads to $\hat{p}_y \hat{k}_z + \hat{p}_z \hat{k}_y = 0$, $\hat{k}_x = \hat{p}_x = 0$ and $\hat{\mathbf{p}} \cdot \hat{\mathbf{k}} = 0$ we have removed the entire contribution from the π_2 (including all interferences with this wave). The solid line corresponds the full calculation (solid line) and the pick at $M_{3\pi} \sim 1.6$ GeV comes almost entirely from the exotic wave since π_2 contribution has been removed. When the exotic is not put into the calculation (dashed line) the remaining small contribution comes from the broad background from the a_1 .

IV. CONCLUSIONS

In this paper we studied the reaction $\vec{\gamma}p \rightarrow X^+n \rightarrow \rho^0\pi^+n \rightarrow \pi^+\pi^-\pi^+n$ for linearly polarized photons at low momentum transfer. We find a qualitative agreement between the data and a theoretical description based on the one pion exchange mechanism, however, more quantitative analysis reveals presence of corrections from absorption and possibly other production mechanisms. The expected dominance of the OPE which fixes naturality in the t -channel enables, through polarization observables to discriminate between naturalities of the produced resonances. Even without full partial wave analysis it turns out to be possible to find maxima in the angular distribution of the $\pi^+\pi^-\pi^+$ system which are dominated by a single resonance. In particular, for exotic, 1^-+ meson production we have shown that there are regions where the contribution from the π_2 meson can be completely eliminated leaving the possibility for the 1^-+ to peak in the intensity. There are other directions where, for example, intensities of the π_2 and a_2 mesons do not contribute. From the formulas in Table 3 more such regions can be found. Of course, this type of analysis cannot be a substitute for the full partial wave analysis, in particular since, as discussed above, other production mechanisms, *e.g.* a natural ρ exchange can modify the

angular distributions. Nevertheless, to the extent OPE does dominate the low- t , charge exchange photoproduction the analysis given here provides a simple filter of the exotic wave.

ACKNOWLEDGMENTS

We thank the members of Hall D Collaboration for stimulating discussions. This work supported by the DOE under contracts, DE-AC05-84ER40150 and DE-FG02-87ER40365.

REFERENCES

- [1] K.J. Juge, J. Kuti, C.J. Morningstar, Nucl. Phys. Proc. Suppl. **63**, 326 (1998); C.J. Morningstar, K.J. Juge, J. Kuti, LANL e-print archive hep-lat/9809098.
- [2] P. Lacock, K. Schilling, LANL e-print archive hep-lat/9809022; C. Bernard *et al.* Phys. Rev. D**56**, 7039 (1997); C. Bernard *et al.* LANL e-print archive hep-lat/9809087; P.Lacock, C. Michael, P. Boyle, P. Rowland, Phys. Lett, B**401**, 308 (1997).
- [3] M. Hess, F. Karsch, E. Laermann, I. Wetzorke, Phys. Rev. D**58**, 111502 (1998).
- [4] D. Horn, J. Mandula, Phys. Rev. D**17**, 898 (1978); K. Yamada, S. Ishida, H. Takahashi, *in proceedings of HADRON 95*, The 6th International Conference on Hadron Spectroscopy, Manchester, Jul 10-14, 1995; A.P. Szczepaniak, E.S. Swanson Phys. Rev. D**55**, 3987 (1997).
- [5] N. Isgur, R. Kokoski, J. Paton, Phys. Rev. Lett. **54**, 869 (1985); N. Isgur, J. Paton Phys. Rev. D**31**, 2910 (1985); E.S. Swanson, A.P. Szczepaniak. Phys. Rev. D**59**, 014035 (1999); P.R. Page, E.S. Swanson, A.P. Szczepaniak, Phys. Rev. D**59**, 034016 (1999).
- [6] T. Barnes, F.E. Close, F.de Viron, J. Weyers, Nucl. Phys. B**224**, 241 (1983); P. Hasenfratz, R.R. Horgan, J. Kuti, J.M. Richard, Phys. Lett. B**95**, 299 (1980); S. Ono, Z. Phys. C**26**, 307 (1984).
- [7] A. Palano, Nucl. Phys. Proc. Suppl. BC **39**, 287, (1995); M. Kunze *et al.* Phys. Atom. Nucl. **57**, 1497 (1994)
- [8] G.S. Adams, *et al.* Phys. Rev. Lett. **81**, 5760. (1998).
- [9] G.T. Condo *et al.*, Phys. Rev. D**48**, 3045 (1993).
- [10] A. Afanasev, P.R. Page, Phys. Rev. D**57**, 6771 (1998).
- [11] N.Isgur, Preprint JLab-THY-99-09, 16pp; E-print Archive: hep-ph/9904494.
- [12] A.Dzierba *et al.* The Hall D Design Report, <http://dustbunny.physics.indiana.edu/HallD>.
- [13] C. Caso *et al.*, Eur. Phys. J. C**3**, 1 (1998).
- [14] K. Schilling *et al.*, Nucl.Phys. B**15**, 397 (1970).
- [15] Y. Eisenberg *et al.*, Phys. Rev. Lett. **23**, 1322 (1969).

TABLES

Resonance	J^{PC}	Mass[GeV]	Partial waves	$\Gamma_{XAB}^{LAB}/\Gamma$	Γ [MeV]	Γ^e [keV]
decay channel						
a_1	1^{++}	1.26			400	640
$\rho\pi$			S	0.99		
			D	0.01		
a_2	2^{++}	1.32			110	295
$\rho\pi$			D	0.70		
rest ($\eta\pi$)			D	0.30		
π_2	2^{-+}	1.67			258	300
$\rho\pi$			P	0.98*0.31		
			F	0.02*0.31		
rest ($f_2\pi$)			S	0.69		
$\hat{\rho}$	1^{-+}	1.6-1.8			100-200	200-600
$\rho\pi$			P	0.50		
rest ($b_1\pi$)			S	0.50		

TABLE I. Resonance parameters used in the model. The numerical values for the widths are taken from the PDG. Γ is the total hadronic width, $\Gamma = \sum_{AB,L_{AB}} \Gamma_{XAB}^{LAB}$ and Γ^e is the total radiative width to $\gamma\pi$.

Resonance	Partial wave	$\frac{(g_{XAB}^{LAB}(k_{AB}(m_X)))^2}{4\pi}$	$\frac{(\bar{g}_{XAB}^{LAB}(k_{AB}(m_X)))^2}{4\pi}$	$\frac{(g_{X\gamma\pi}^{L\gamma})^2}{4\pi}$
a_1				
$\rho\pi$	S	26.28	18.70	1.03
	D	32.54	23.15	1.04×10^{-2}
a_2				
$\rho\pi$	D	443.4	563.48	2.37
rest ($\eta\pi$)	D	57.08	72.71	
π_2				
$\rho\pi$	P	20.01	15.54	1.74
	F	20.15	15.64	4.01×10^{-2}
rest ($f_2\pi$)	S	13.72	10.65	
$\hat{\rho}$				
$\rho\pi$	P	24.59	20.85	1.51
rest ($b_1\pi$)	S	7.12	6.04	

TABLE II. Strong, physical and physical and electromagnetic couplings as defined in text. The strong couplings are evaluated for $\Lambda = 1$ GeV. The physical couplings are obtained from the BW widths given in Table 1 and then the bare couplings are calculated using Eq. (11). For the 1^{-+} we used $\Gamma = 170$ MeV and $\Gamma^e = 400$ keV.

Resonance	Partial wave	$W(\theta_k, \phi_k, \theta_p, \phi_k)$
a_1	S	\hat{p}_y^2
	D	$\left(\hat{k}_y \hat{\mathbf{p}} \cdot \hat{\mathbf{k}} - \frac{\hat{p}_y}{3}\right)^2$
a_2	D	$\left(\hat{k}_z [\hat{\mathbf{k}} \times \hat{\mathbf{p}}]_x + \hat{k}_x [\hat{\mathbf{k}} \times \hat{\mathbf{p}}]_z\right)^2$
π_2	P	$(\hat{p}_y \hat{k}_z + \hat{p}_z \hat{k}_y)^2$
	F	$\left(\hat{k}_z \hat{k}_y (\hat{\mathbf{p}} \cdot \hat{\mathbf{k}}) - \frac{\hat{k}_z \hat{p}_y + \hat{p}_z \hat{k}_y}{5}\right)^2$
$\hat{\rho}$	P	$\left([\hat{\mathbf{k}} \times \hat{\mathbf{p}}]_x\right)^2$

TABLE III. Unnormalized angular decay distributions of the $\pi^+(-\mathbf{p})\pi^-(\mathbf{p})\pi^+(\mathbf{k})$ for photons polarized in the direction perpendicular to the production plane (\mathbf{y}). The angular distributions corresponding to photons polarized along \mathbf{x} are obtained by interchanging the subscripts $y \rightarrow x$ and $x \rightarrow y$ in the third column.

FIGURES

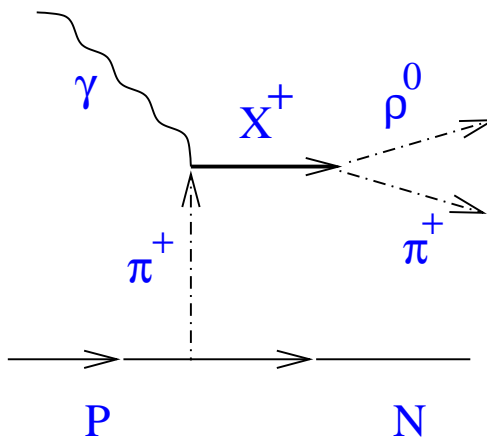


Fig. 1. $\rho^0\pi^+$ photoproduction via one-pion-exchange.

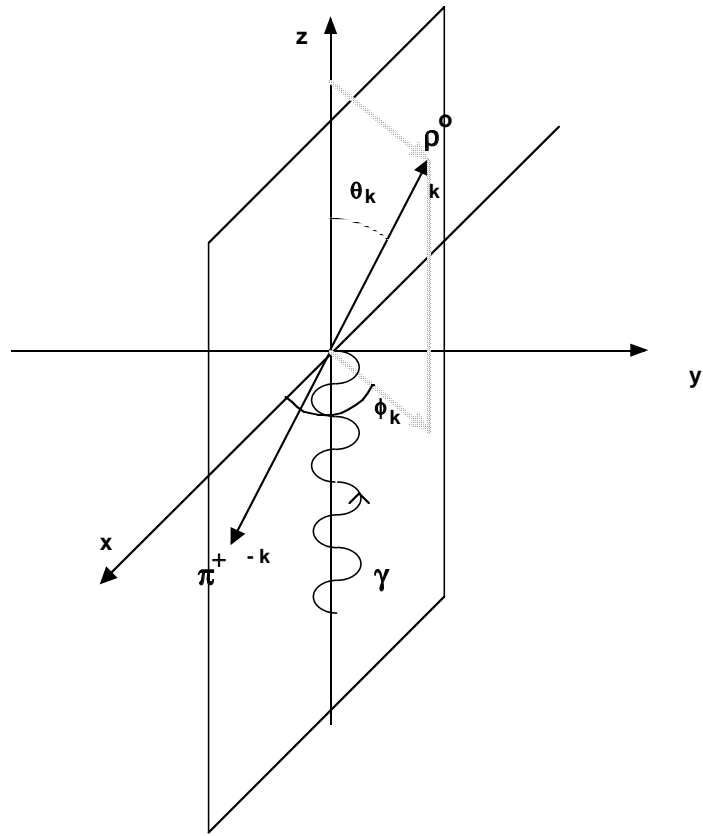


Fig. 2. Kinematics of the $\rho^0 \pi^+$ production in the GJ frame.

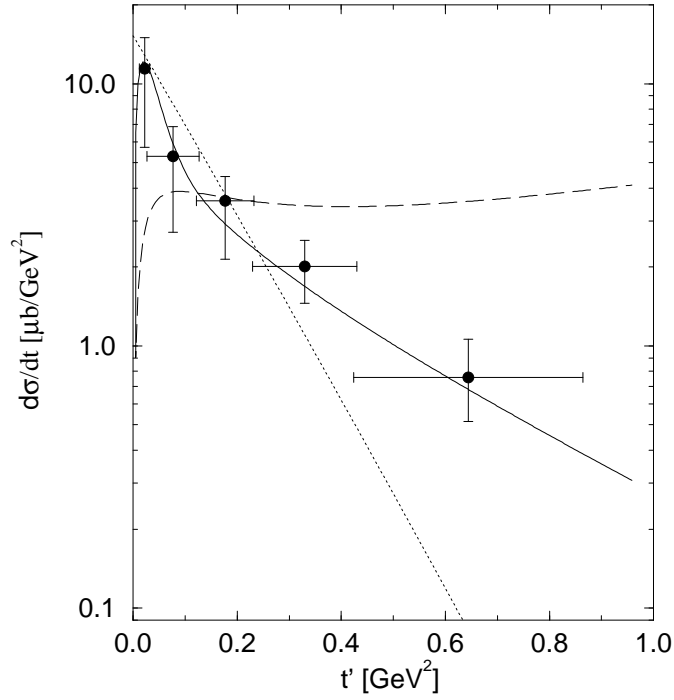


Fig. 3. Momentum transfer dependence of a_2^+ photoproduction cross section. Data is from Ref. [15]. Solid line is the OPE prediction corrected to account for absorption. Dashed line is the pure OPE prediction and the dotted line is the $A \exp(-bt)$ parameterization.

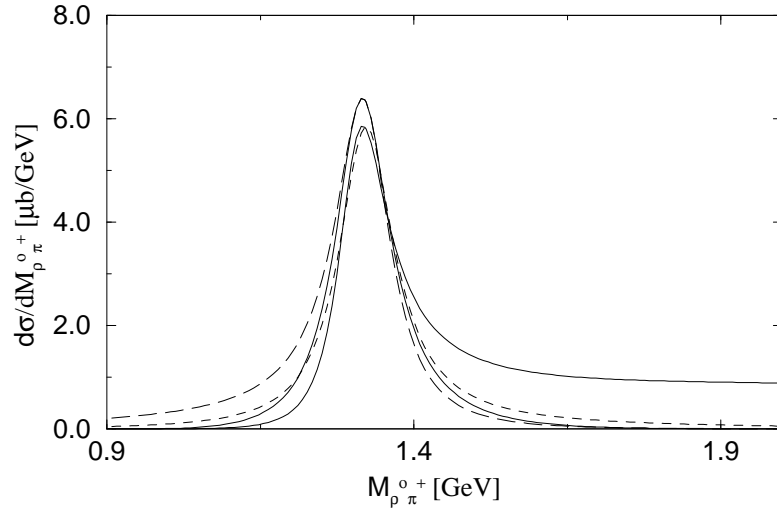


Fig. 4. $\rho^0\pi^+$ photoproduction cross section through a single a_2^+ resonance. The various curves are explained in the text.

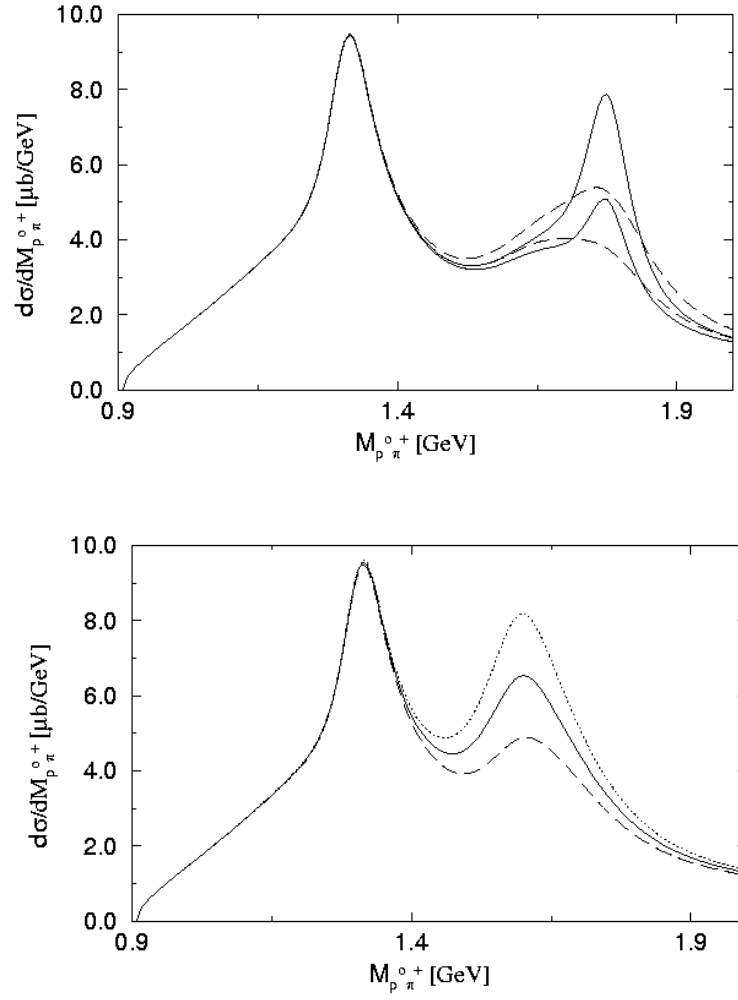


Fig. 5a,b. $\rho^0\pi^+$ photoproduction cross section via with the contributions from a_1 , a_2 , π_2 and a 1^{-+} exotic state for different widths of the exotic resonance for a) $M_{1^{-+}} = 1.775$ GeV and b) $M_{1^{-+}} = 1.6$ GeV.

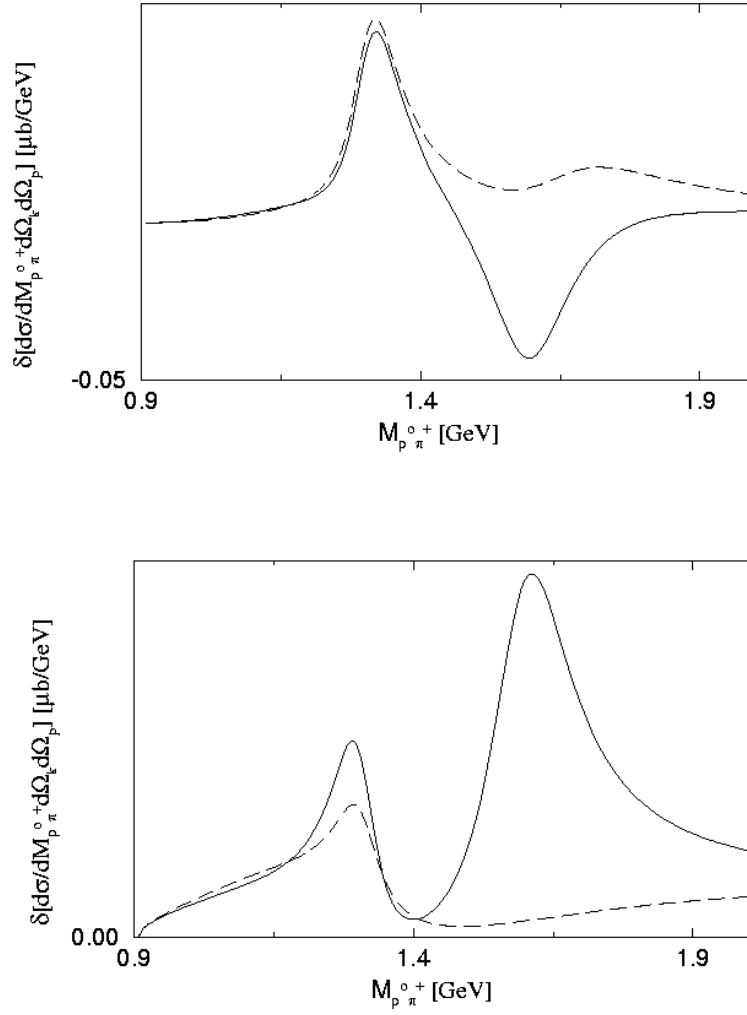


Fig. 6a,b. $\delta d\sigma/dM_{p^0 \pi} + d\Omega_p d\Omega_k$ for linearly polarized photons along-x and along-y at a) $|k_x| = |k_y|$, $\hat{\mathbf{p}} \cdot \hat{\mathbf{k}} = 0$, $\theta_p = 0.35\pi$ and b) $\hat{\mathbf{p}} \perp \hat{\mathbf{k}}$, $k_x = 0$, $\theta_k = \pi/4$.